ACCEPTED FOR PUBLICATION IN ApJ
Preprint typeset using LATEX style emulateapj

THE S-PROCESS IN METAL-POOR STARS: ABUNDANCES FOR 22 NEUTRON-CAPTURE ELEMENTS IN CS 31062-050

JENNIFER A. JOHNSON
Dominion Astrophysical Observatory, Herzberg Institute of Astrophysics, National Research Council of Canada, 5071 West Saanich Rd., Victoria, BC V9E 2E7, Canada

AND

MICHAEL BOLTE
UCO/Lick Observatory, University of California, Santa Cruz, CA 95064

accepted for publication in ApJ

ABSTRACT

The CH star CS 31062-050 ([Fe/H] = –2.42) is one of the most useful stars yet discovered for evaluating the s-process in metal-poor stars. It is very abundant in heavy elements (e.g., [La/Fe] = 2.2), and its relatively cool temperature and low gravity mean that there are many lines of interesting elements present in the spectrum. We measured the abundances of 22 elements with Z$\geq$29, including the rarely measured Lu and Pd. We derive an upper limit on the Th abundance as well. The abundances in CS 31062-050 show a similar pattern to many other metal-poor CH stars: high [Pb/Fe] and [Pb/La] ratios, low [Y/La] ratios and high [Eu/La] values compared to the solar system s-process. However, the Th limit, with additional assumptions, is not consistent with the idea that the excess Eu in CS 31062-050 is contributed by the r-process. In addition, the observed [Eu/Tb] cannot be explained by any ratio of solar-system s-process and r-process abundances. We therefore argue that the abundance pattern in CS 31062-050 is most likely the result of the s-process, and we discuss possible modifications that could explain the non-solar-system pattern observed.

Subject headings: nuclear reactions, nucleosynthesis, abundances, stars:abundances — stars: atmospheres — stars: Population II

1. INTRODUCTION

The sample of identified field stars with [Fe/H][1]< -2.4 has increased by more than an order of magnitude in the last decade. Because the elements in the atmospheres of these stars have been produced in a small number of nucleosynthetic events, abundance determinations can provide direct tests of model yields from different nuclear processes. Even in the early work on very metal-poor stars it quickly became clear that there were subclasses of objects with very high [heavy-element/Fe] ratios that could be traced to specific nucleosynthetic origins (e.g., McWilliam et al. 1995).

The elements heavier than the iron peak are made through neutron capture via two principal processes: the r-process and the s-process (Burbidge et al. 1957). The r-process (for rapid process) occurs when neutrons are added much more rapidly than the β decay times of the relevant nuclei. The site or sites of the r-process are not known, although suggestions include the ν-driven wind of Type II SNe (e.g., Woosley & Hoffman 1992; Woosley et al. 1994) and the mergers of neutron stars (e.g., Lattimer & Schramm 1974; Rosswog et al. 2000). The s-process occurs when neutrons are added more slowly and β decays, changing neutrons to protons, keep the nuclei from straying far from the valley of β stability. The He intershell in asymptotic giant branch (AGB) stars is the site of the s-process as well as of C production. C and heavy elements are brought to the surface of the AGB stars during the "third dredgeup". Since the r-process produces very neutron-rich nuclei initially, the r-process reaches the neutron magic numbers with considerably fewer protons than the s-process, and, as a result, these two processes produce abundance peaks at different atomic weights. As a result, when the solar-system total abundances (t_{ss}) are separated into contributions from the s-process (s_{ss}) and the r-process (r_{ss}) (e.g., Käppeler, Beer, & Wisshak, 1989; Arlandini et al. 1999), some elements are mostly contributed by the r-process, such as Eu, and some by the s-process, such as Ba and La. Therefore Eu is commonly referred to as an "r-process element" and Ba and La as "s-process elements". The [Eu/Ba] and the [Eu/La] values are used to estimate the ratio of r-process to s-process contributions to the heavy element abundances in a star, increasing as the r-process fraction increases. Despite the nomenclature, it is important to remember that all neutron-capture elements lighter than Z=84 are made in both processes (Clayton & Rassbach 1967). Th (Z=90) and U (Z=92) can only be made in the r-process.

The surveys of metal-poor stars have uncovered stars rich in C and s-process elements and stars rich in r-process elements. These have been the subject of many follow-up studies, because of the insight they can provide on the production of the heavy elements in the early Galaxy.

1.1. *The very metal-poor CH stars*

Metal-poor stars with enhanced abundances of C and s-process elements are called CH stars. In an extensive survey, McClure (1984) and McClure & Woodsworth (1990) showed that all of the CH stars in their sample were members of binary systems with orbital parameters consistent with a white dwarf secondary. The explanation for the classic CH stars is that they result from the transfer of C, N, and s-process material produced in an AGB companion which is now a white dwarf. The abundance patterns in CH stars for the heavy elements are therefore a very accessible means of empirically de-

[1]We use the usual notation [A/B]$\equiv \log_{10}(N_A/N_B)_* - \log_{10}(N_A/N_B)_\odot$ and $\log\epsilon(\mathrm{A}) \equiv \log_{10}(\mathrm{N_A/N_H}) + 12.0$. A/B$\equiv N_A/N_B$.

riving s-process yields and for inferring the structure of, and physical conditions in, AGB stars. The traditional indicators of s-process material are super-solar [Ba/Fe] (the Pop I version of CH stars are often referred to as barium stars) and subsolar [Eu/Ba].

Theory predicts that s-process nucleosynthesis will depend on the initial metallicity of the AGB star and on its mass (Gallino et al. 1998; Goriely & Mowlavi 2000; Busso et al. 2001). Busso et al. reported s-process yields as a function of initial [Fe/H] and for AGB stars with 1.5 and 3.0$M_\odot$ and made comparisons with the available observational data. The basic metallicity dependence is a tilting of the s-process products toward heavier elements with decreasing [Fe/H] of the host AGB star. The prediction that ^{208}Pb will have a particularly strong excess has been verified for CS 22183-015 (Johnson & Bolte 2002a), HE 0024-2523 (Lucatello et al. 2003) and many of the stars studied by Van Eck et al. (2001, 2003) and Aoki et al. (2002) (A02). On the other hand, Aoki et al.(2000, 2001) present the analysis of two metal-poor, s-process-rich stars, LP 625-44 and LP 706-7, which have [Pb/Ba] $\sim$ 0.

1.2. *Very metal-poor r-process-rich stars*

There is a second class of neutron-capture-rich very metal-poor stars in which the abundance pattern of the heavy elements more closely follows that inferred for the r-process elements in the solar system. CS 22892-052 (Sneden et al. 1996, 2000), HD 115444 (Westin et al. 2000) and CS 31082-001 (Cayrel et al. 2001) are the best studied members of this class. Studies have showed a remarkable similarity in the abundance ratios for elements between Ba (Z= 56) and Hf (Z= 72), (c.f. Truran et al. 2002) although in the lighter and heavier r-process element peaks there is considerable star-to-star scatter in abundance ratios (e.g., Sneden et al. 2000; Johnson & Bolte 2002b; Hill et al. 2002). Some r-process-rich stars, in particular CS22892-052, are also C-rich. The source of that C is unknown. Finally, we note that very metal-poor stars with low [neutron-capture/Fe] ratios have abundance patterns between Ba and Hf that agree with r_{ss} (Sneden & Parthsarathy 1983; Gilroy et al. 1988; Johnson & Bolte 2001).

1.3. *Some puzzles and challenges*

As more detailed studies of very metal-poor CH stars became available, some stars and elements did not fit neatly into the picture described above. Despite having lower [Eu/Ba] than the r-process-element-rich stars, in some CH stars [Eu/Ba] is higher than that s_{ss} or than predicted for the metal-poor s-process. Hill et al. (2000) analyzed spectra of two CH stars, CS 22948-027 and CS 29497-034, and concluded that the observed abundances could not be fit by either a scaled solar-system s-process (s_{ss}) or scaled solar-system r-process (r_{ss}), but instead reflected enrichment by both processes.

A02 and Johnson & Bolte (2002a) also noted a large spread in [Eu/Ba] for other CH stars but suggested that the abundance pattern seen in these CH stars was due solely to the s-process, albeit one that produces a varying Eu/Ba ratio. A large percentage of CH stars have Eu/Ba ratios larger than s_{ss}. With the Hill et al. interpretation, this would suggest that a number of s-process-rich stars are also r-process rich. Some fraction of non-CH field stars are Eu-rich, so it would not be surprising to find some stars that began as r-process-rich and also were polluted by an AGB companion later in their lives. However, while seven of 32 non-CH stars in McWilliam et al. (1995) have [Eu/Fe] $\gtrsim$ 0.5, six of eight CH stars in A02 have such high Eu. So it appears that r-process enrichment cannot be the solution for *all* the high Eu CH stars (but see below).

Recently, Cohen et al. found an extreme example of non-s_{ss} ratios in the CH star HE 2148-1247. The measured Ba/Eu ratio was $\sim$ 100 while theoretical calculations from Arlandini et al. (1999), for example, give Ba/Eu $\sim$ 640. They favored the addition of r-processed material as well as s-processed material to HE 2148-1247. Qian & Wasserburg et al. (2003), in a companion paper, proposed an intriguing theory for the creation of such "s+r"-process stars. First some s-processed material is accreted from the AGB companion, which turns into a white dwarf. Later in the evolution of the system, the white dwarf accretes matter from the polluted star and suffers an accretion-induced collapse (AIC) to a neutron star. The ν-driven wind produces an r-process, which also pollutes the companion, but since the white dwarf lacks an H or He envelope, lighter elements, such as Fe, are not manufactured. Therefore, the remaining star is r-process *and* s-process-rich. The AIC could potentially deliver a strong kick to the neutron star, which could explain why some CH stars have recently been shown not to be members of binaries (Preston and Sneden 2001; Hill et al. 2000). Because the production of the s-process in the AGB star and the production of the r-process in the AIC are connected to the same binary companion, this alleviates some of the concern expressed by A02 and Johnson & Bolte (2002) about the high frequency of potential s+r stars. However, at least 50% of the very metal-poor CH stars would need to be s+r stars if that is the explanation for the elevated Eu/Ba ratios (see Figure 13 in Cohen et al. (2003)). As Qian & Wasserburg point out, the frequency of AIC events and the parameters necessary to create them are unknown at this time, but the large fraction of very metal-poor CH stars with high Eu implies that the ability to pollute a companion as a AGB star must be tightly correlated with an r-producing AIC event. Another possible problem these authors mention is the still uncertain nucleosynthesis in AIC, which may or may not produce the r-process.

If we hope to understand the origin of neutron-capture elements in CH stars, we need to measure the abundances of as many heavy elements as possible to see if they are consistent with an s+r, or s-only or r-only scenario. In this paper, we present results for another CH star. Because of the combination of large abundance enhancements and atmospheric parameters in this star, we can measure accurate abundances for a number of elements that have been infrequently studied in CH stars. These include Pd, Tb, Ho, Tm and Lu. We have also been able to put interesting limits on the abundance of Th.

2. OBSERVATIONS

CS 31062-050 was selected from a survey of metal-poor star candidates that we have undertaken with the Keck 2 telescope and the intermediate-resolution echelle spectrometer ESI (Sheinis et al. 2002). The goal of the ESI program is to obtain the abundances of Fe, Ti, Mg, Ca, Ba and in some cases Eu for very metal-poor star candidates and to identify interesting targets for follow-up at higher resolution and bluer wavelengths with Keck 1 and HIRES (Vogt et al. 1994). CS 31062-050 was identified as a metal-poor star candidate by the UBV photom-

etry of Norris, Ryan & Beers (1999). An ESI spectrum was obtained on 29 August 2000. A single 900s exposure gave a high S/N (> 100) spectrum at R$\sim$ 7000 from 3900Å to 1μm. The high carbon abundance of CS 31062-050 was immediately evident from the strength of the G-band. The ESI spectrum also revealed strong Ba II and Eu II lines. We took higher-resolution spectra with HIRES on Keck I on 25 and 26 August 2001. A 0$''$.86 slit gave R$\sim$45,000. A blue setting which covered the wavelength 3190Å–4710Å was used for three observations of 1800s each. The second grating setting covered 3730Å–5275Å and was also used for three observations of 1800s. Exposures of a quartz lamp were used for flatfielding and of a ThAr lamp for wavelength calibration. The frame processing was done in IRAF[2]. In addition to combining the three observations at each setting, we also combined all six observations together where they covered the same wavelengths. Our S/N ranged from $\sim$ 10 at 3200 Å to $\sim$80 at 4000Å to $\sim$ 100 at 5250Å. This star was also studied by A02, but at lower S/N and without the very blue wavelength coverage. They found that this star was extremely C- and N-rich, with [C/Fe]= 2.0 and [N/Fe]= 1.2 We were able to measure the abundances of several neutron-capture elements not included in the A02 study, and these provide interesting tests for theories of the origin of the heavy elements in the early Universe.

3. ABUNDANCE ANALYSIS

MOOG (Sneden 1973) was used for the abundance analysis. We used Kurucz[3] (2003) model atmospheres. Our $T_{\rm eff}$ comes from the excitation equilibrium of Fe I lines. Deriving $T_{\rm eff}$ from colors in carbon-rich stars can be problematic because the presence of a large number of molecular lines affects the observed colors. However Hill et al. (2000) found that their excitation equilibrium temperature was consistent with temperatures derived from colors when they included the effects of the molecular lines on the atmospheres and on the colors. Our gravity comes from ionization equilibrium of Fe I/Fe II. The validity of this assumption in view of possible NLTE effects on Fe I lines has been the subject of much recent discussion (see e.g., Lucatello et al. 2003; Johnson 2002), but the abundances of most of the heavy elements are affected in the same manner by a change in log g. The microturbulent velocity (ξ) was determined by requiring Fe I lines of different equivalent widths (EWs) to give the same [Fe/H]. Our final atmospheric parameters are $T_{\rm eff}$=5500K, log g=2.70, ξ=1.3 km/s and $[{\rm Fe/H}]_{mod}$ = –2.30. These agree well with the parameters adopted by A02 for this same star ($T_{\rm eff}$=5600K, log g=3.00 and ξ=1.3 km/s). This implies too low a luminosity for this star to be an AGB star. We also checked for the presence of Tc lines at 4049Å and 4088Å using the atomic parameters from Vanture et al. (1991). No Tc was detected, which supports our conclusion that this not a self-polluting AGB star, although large Tc enhancements would be required for any lines to be visible. Finally, Aoki et al. (2003) have found radial velocity variations in this star. We conclude that CS 31062-050 is a CH star.

We selected a number of lines with good gf-values. Whenever possible, we used recent laboratory measurements. Our choices for gf-values for the heavy elements are summarized in the Appendix. Hyperfine splitting (HFS) and isotopic splitting (IS) are important for many lines of the heavy elements, and we included them for all the elements with HFS and IS constants for the relevant levels in the literature. These sources are discussed in the Appendix as well. For elements lighter than Cu, we used the linelists of Johnson (2002).

The large enhancements of neutron-capture elements meant that we could measure many lines of heavy elements, including some not identified in the solar atlas of Moore, Minnaert & Houtgaust (1966) or in previous abundance analyses of metal-poor stars. To find other lines that would be useful for abundance analysis, we created lists of all the lines from our sources of gf-values. We then predicted their EWs using MOOG. For lines with EWs $>$ 5mÅ (slightly more for the lower S/N regions), we synthesized the region. Our starting point was the Kurucz & Bell (1995) (KUR95) line lists, which contained many rare earth lines that are the true contaminants in this situation, but were unimportant in the Sun and not included in Moore et al.. For lines we wanted to use for abundance analysis, we checked for blends from other lines and only used a line if it were essentially unblended or if the other line contributing to the blend had a recent, laboratory-based gf-value. We also synthesized the regions in three metal-poor stars: HD 122563 (neutron-capture and C-poor) (e.g., Westin et al. 2000), CS 22183-015 (neutron-capture and C-rich) (Johnson & Bolte 2002), and CS 22957-027 (neutron-capture-poor and C-rich) (e.g., Norris, Ryan, & Beers 1997) to check that our linelists adequately accounted for contamination from atomic and molecular lines. Our EWs and atomic parameters are in Table 1. We compared our EWs to those of A02 for the 22 lines we had in common. We found an average offset of –0.8mÅ with an r.m.s. scatter of 5.9 mÅ, indicating excellent agreement between the two studies. Below we include some notes on three of the most interesting or uncertain abundances.

3.1. *Palladium*

A rarely measured element is the intermediate-mass neutron-capture element Pd. With A$\sim$130, it lies between the better-studied regions near Sr (A$\sim$90) and Ba (A$\sim$160). When this region was first explored in metal-poor r-process-rich stars, unexpected deviations from r_{ss}were found (Sneden et al. 2000 ; Johnson & Bolte 2002b). Of all the elements in this mass region, we could measure one line of Pd. Our synthesis is shown in Figure 1. The gf-value is from Biémont et al. (1982) and the line list is from Johnson & Bolte (2002b). Unfortunately, none of the odd elements in this mass region, such as Ag, could be measured because their lines are weaker than that of Pd and they are in regions of the lower S/N.

3.2. *Lutetium*

We were able to detect the 3507.4Å line of Lu II in CS 31062. It has a very accurate gf-value and HFS constants from the study by Den Hartog et al. (1998). It is blended in CS 31062-050 with an Fe II line. This Fe II line has a gf-value from Moity (1983). Figure 1 shows our synthesis of the Lu II line. The hyperfine splitting of the Lu line is significant enough to noticeably broaden the line. Figure 1 shows that no amount of absorp-

[2]IRAF is distributed by the National Optical Astronomy Observatories, which are operated by the Association of Universities for Research in Astronomy, Inc., under cooperative agreement with the National Science Foundation

[3]http://cfaku5.harvard.edu/

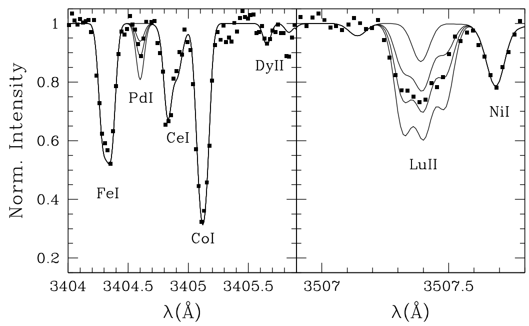

FIG. 1.— Spectral synthesis of (left) Pd I and (right) Lu II in CS 31062-050. The solid squares are the data. The solid lines represent, in order of increasing strength and relative to our adopted log ϵ = $-\infty$, –0.3 dex, 0.0 dex, and +0.3 dex. Several lines in these regions of the spectrum have uncertain gf-values and we have increased the gf-value for Fe I on the left and Ni I on the right above that in KUR95 to fit the spectrum.

tion from Fe II will account for the profile of the observed line, while the three components of the Lu II line are a good match when the S/N is taken into account.

3.3. *Thorium*

A possible detection of the r-process-only element Th was one of the reasons that Cohen et al. (2003) favored an s+r scenario. Unfortunately, in CS 31062-050 the strongest Th line at λ4019Å is blended with a ^{13}CH line (Norris, Ryan, & Beers 1997). Because we could only set large upper limits ([Th/Fe]$<$ 3.0) using the non-detection of other, non-blended Th lines in our spectra, we decided to use the line at 4019Å. The linelist from Johnson & Bolte (2001) was used, except our gf-value for the Th II line was revised up by 0.05 dex to reflect the recent laboratory measurement of the oscillator strength by Nilsson et al. (2002). The Ce II line noted by Sneden et al. (1996), which in our previous work was an unimportant contributor to the absorption, is much more important in this s-process-rich star. Our fit to the left of the Th line was improved if we shifted the Ce II line by 0.02Å to the red from its position in Johnson & Bolte (2001) and its gf-value decreased by 0.1 dex. This was a cosmetic change and does not affect the Th abundance determination. In an attempt to test the goodness of the fit of our synthesis spectra with different Th abundances, we did a χ^2 test of the wavelength region of 4019.08–4019.25Å. The errors in our data points were assumed to be solely due to the Poisson noise in the counts, The smoothing of the synthesis was set by other lines in the region and not allowed to vary. The C abundance was set to match the ^{12}CH lines at 4020Å ([C/Fe]=1.82), and a ^{12}CH/^{13}CH value of 12 was used. We find a 3σ limit of log $\epsilon(Th)$ = –0.85 and a 5σ limit of log $\epsilon(Th)$ = $-$0.70. Our syntheses for these limits are shown in Figure 2.

4. RESULTS

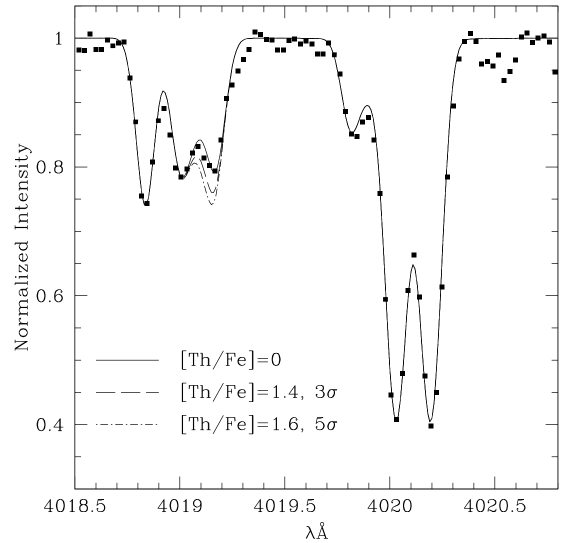

FIG. 2.— Spectral synthesis of the Th line at 4019Å. The solid squares are the data. At [Th/Fe]=0, the Th line is so weak that our synthesis is indistinguishable from a synthesis with no Th.

Our abundances and errors are in Table 2. The solar values are adopted from the meteoritic abundances in Grevesse, Noels, & Sauval (1996). Table 2 also includes a comparison with the A02 abundances. Our lower $T_{\rm eff}$ and gravity mean that we have lower logϵ in general for the singly-ionized rare earth species, but the offset from A02 is fairly constant. The abundances of the elements between Mg and Ni are in good agreement with metal-poor field stars that are not C-rich or heavy-element-rich studied with the same linelist by Johnson (2002). The "α"-elements (Mg, Ca, and Ti) have supersolar [X/Fe] ratios. The iron-peak elements track Fe closely with the exception of Mn, whose depletion relative to iron in metal-poor stars was first noted by McWilliam et al. (1995). Therefore, any explanation of the over-enhancements of the neutron-capture elements cannot change the lighter elements away from the standard halo patterns. [Cu/Fe] and [Zn/Fe] in CS 31062-050 agree with the trends seen in the majority of metal-poor stars (Sneden, Gratton, & Crocker 1991; Primas et al. 2000).

In Figure 3, we plot the abundances of CS 31062-050 as well as r_{ss}, s_{ss}, and t_{ss} scaled to match the abundance of La. We use La rather than the more traditional Ba because of the large uncertainties in measuring the Ba abundance (see Appendix). It is clear that none of t_{ss}, s_{ss} or r_{ss} is a good match to the data. In several respects, s_{ss} is the closest, particularly for explaining elements like La, Ce, Pr, Nd, Tb, Dy, and Ho. However, while Y and Zr are enhanced relative to the majority of metal-poor stars, they are not as abundant as a simple scaling of s_{ss} implies. Pd is also $\sim$ 1 dex below the solar system lines. Pb, on the other hand is above the solar system lines with [Pb/Fe]=2.81 and [Pb/La]=0.69. Although this value is not as extreme as CS 22183-015 (Johnson & Bolte 2002a) or the stars in Van Eck et al.(2001), it is supersolar.

We can understand this tilt toward heavier nuclei as the result

TABLE 2
ABUNDANCES

Ion	log ϵ	[X/Fe][a]	σ	σ_{tot}	N_{lines}	Δ A02[b]
Mg I	6.01	0.84	0.20	0.21	1	
Ca I	4.43	0.49	0.10	0.09	2	
Ti I	2.85	0.32	0.25	0.13	9	
Ti II	2.86	0.33	0.10	0.23	4	
V II	1.44	–0.17	0.14	0.18	2	
Cr I	3.36	0.08	0.19	0.15	3	
Mn I	2.69	–0.43	0.12	0.12	4	
Fe I	5.09	–2.41	0.11	0.13	46	–0.10
Fe II	5.10	–2.40	0.13	0.15	10	–0.07
Co I	2.60	0.10	0.20	0.23	1	
Ni I	3.68	–0.16	0.17	0.21	11	
Cu I	0.69	–1.19	0.20	0.18	2	
Zn I	2.32	0.06	0.20	0.23	1	
Y II	0.30	0.48	0.10	0.22	14	
Zr II	1.05	0.85	0.14	0.19	9	–0.26
Pd I	0.27	0.98	0.20	0.24	1	
Ba II	2.61	2.80	0.20	0.19	3	0.40
La II	0.93	2.12	0.12	0.19	25	–0.41
Ce II	1.24	2.02	0.16	0.18	36	–0.17
Pr II	0.13	1.74	0.11	0.16	10	
Nd II	1.07	1.99	0.18	0.22	39	–0.34
Sm II	0.53	1.96	0.14	0.18	12	–0.28
Eu II	–0.07	1.79	0.07	0.17	5	–0.14
Gd II	0.51	1.83	0.12	0.19	24	
Tb II	–0.56	1.50	0.10	0.16	4	
Dy II	0.39	1.63	0.07	0.23	20	–0.54
Ho II	–0.40	1.55	0.16	0.18	3	
Er II	0.78	2.22	0.13	0.26	15	
Tm II	–0.29	1.97	0.10	0.19	4	
Yb II	0.76	2.21	0.20	0.30	1	
Lu II	–0.10	2.18	0.20	0.26	1	
Hf II	0.67	2.33	0.10	0.20	11	
Pb I	2.46	2.81	0.15	0.15	2	–0.14

[a][X/Fe] for all elements except Fe, where [Fe/H] is given

[b]$\log\epsilon_{thisstudy} – \log\epsilon_{A02}$

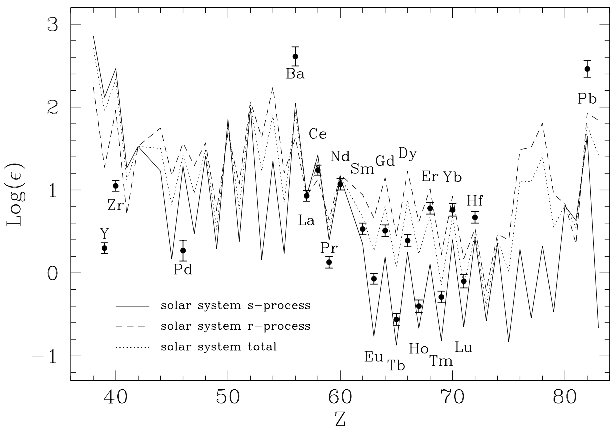

FIG. 3.— The abundance in CS 31062-050 compared with s_{ss}, r_{ss}, and t_{ss}. In all cases the solar abundances were scaled to match the La abundance of CS 31062-050. No solar abundance pattern is a good match to the data, even in a limited Z range.

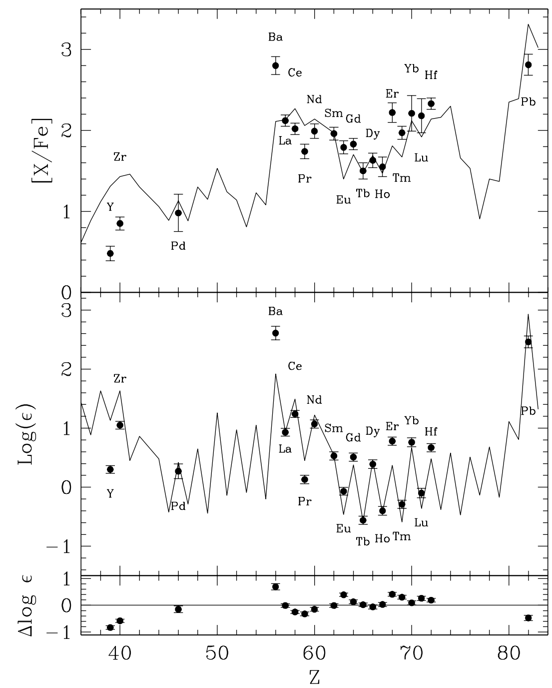

FIG. 4.— The abundance in CS 31062-050 (filled circles) compared with an s-process calculation for a metal-poor AGB star. The top panel shows [X/Fe], which highlights the rise in over-abundances of the neutron-capture elements as Z increases. The middle panel shows log ϵ vs. Z, which shows that the metal-poor s-process model does a better job of fitting the data than scaled solar system abundance patterns, although Eu and Er are both underpredicted. The difference between the model and the data is shown in the bottom panel.

of a high neutron-to-seed ratio (Gallino et al. 1998). Figure 4 shows the abundances in CS 31062-050 compared with the results of an s-process in a $1.5 M_{\odot}$ AGB star with [Fe/H]= –2.3. (R. Gallino, private communication). The top panel of Figure 4 shows the steep rise in [El/Fe] as Z increases, which is matched much better by the metal-poor s-process than by s_{ss}, although Y and Pb are not simultaneously fit. However, the agreement with Pd, Sm, Tb, Dy and Ho is very encouraging and a marked improvement over Figure 3. The bias to heavier nuclei can also be quantified using the light s-process to heavy s-process ratio [ls/hs]. The value for CS 31062-050 (using the elements suggested by Busso et al., 2001) is 1.39, in good agreement with predictions for the s-process in [Fe/H]$\sim$ –2.5 AGB stars and with other observations of CH stars (Busso et al. 2001). This model predicts no appreciable production of Cu or Zn. The low Cu and Zn observed in CS 31062-050 (Table 2) are also consistent with the conclusions of Matteucci et al. (1993) that Cu is primarily made in either explosive nucleosynthesis or the weak s-process and Zn in explosive nucleosynthesis, because they are clearly not made in the AGB star that polluted CS 31062-050.

The most glaring misfits in the Z$\geq$ 56 range are the abundances of Eu and Er (and, with larger error bars, Ba). It was a similar observation, in particular the high Eu abundance, that prompted the suggestions of Hill et al. and Cohen et al. (2003) that CH stars with this characteristic were rich in both the s- and r-process. We now examine this question in more detail.

5. SOURCES FOR THE HEAVY ELEMENTS IN CS 31062-050

There are now a number of very metal-poor CH stars with high-resolution abundance analyses. A surprising number of them have [Eu/La] too high to be consistent with s_{ss} (Figure 5). Since Eu is predominately produced in the r-process in the solar system, the r-process is an clear choice for the source of Eu in CS 31062-050. If the r-process contributes an appreciable amount to the heavy elements then we would expect relatively high abundances of elements mostly or only produced in the r-process. Unfortunately, we could only obtain uninteresting upper limits for elements in the third r-process peak such as Os and Ir. However, the limit for Th, an r-only element, is more interesting.

5.1. *Thorium abundance?*

We found an 3σ upper limit to the abundance of Th of logϵ = –0.85. What does this tell us about the possible contributions of the r-process to the lighter neutron-capture elements, such as Eu? We cannot definitely predict the expected Eu abundance in CS 31062-050 from the Th abundance since the ratio between Eu and the initial Th value produced in the r-process is not always constant. One theoretical calculation predicts Th/Eu=0.496 (Cowan et al. 1999), and many stars show that to be a reasonable value (Sneden et al. 2000; Johnson & Bolte 2001; Cowan et al. 2002). While CS 31082-001 (Hill et al. 2002) clearly disagrees with this Th/Eu ratio, its implied Th/Eu$_{initial}$ is higher than the value we use here, which would only decrease the possible contribution to the r-process to the Eu abundance derived from our Th limit. If we use Th/Eu=0.496 and an age for CS 31062-050 of 14 Gyr, we

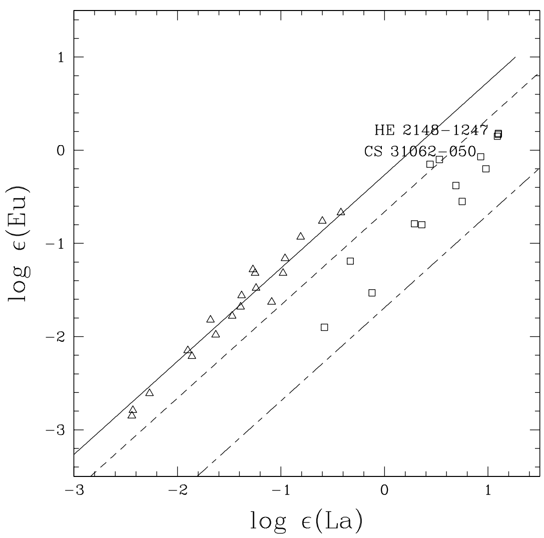

FIG. 5.— Log ϵ(Eu) vs. log ϵ(La) for a sample of CH (squares) and non-CH stars (triangles) with [Fe/H]< –2.0. The lines represent an r_{ss} ratio (solid), s_{ss} ratio (dot-dash) and t_{ss} ratio (dashed) of La to Eu. The non-CH stars are identified by their adherence to the r_{ss} line and have a wide range of Eu (and C) abundances. The CH stars have a wide range of La/Eu ratios and large enhancements in both elements.

find that at most 66% of our Eu abundance could come from the r-process. We can now perform the same calculation for the s-process contribution, using the observed La/Eu ratio and the solar system s-process ratio from Arlandini et al. (1999). Here we find that the s-process only contributes 23% of the Eu, leaving at least 10% of the Eu without a source. Either our assumed s-process or r-process ratios are incorrect. Clearly, more r-process-rich stars with Th determinations will eventually better constraint the possible (Th/Eu)$_{initial}$ range, but based on current data, our upper-limit on Th argues against the r-process as the solution to the abundance pattern in CS 31062-050.

5.2. *[Eu/Tb]*

The ratio of the predominately r-process elements Eu and Tb provide even stronger evidence that no combination of r_{ss} and s_{ss} or current models for the metal-poor s-process can fully explain the abundnaces measured in CS 31062-050. According to Arlandini et al. (1999), 94.2% of the solar system Eu is due to the r-process as is 92.8% of the solar system Tb. Therefore, only a small variation in the ratio of Eu/Tb can be produced if we confine ourselves to the solar system patterns. A pure r-process results in Eu/Tb of 1.52, and a pure s-process results in Eu/Tb of 0.625. Neither pure s_{ss} nor pure r_{ss} nor any combination of those two can create the Eu/Tb=3.1 that we measure in CS 31062-050. These predictions for r_{ss} for Eu and Tb are the result of subtracting s_{ss} from the total solar abundances, so the predictions for the two processes are correlated. In this case, given the overwhelming proportions of Eu and Tb produced in the r-process in the solar system, changing s_{ss} will not affect r_{ss} significantly, and so our argument that the r-process is not responsible is robust against changes in s_{ss}. In addition, the Busso et al. (2001) metal-poor s-process models predict similar abundances of Eu and Tb. Therefore any combination of these models and r_{ss} also will fail to reproduce the high Eu/Tb value. Could observational error explain the large [Eu/Tb] ratio? We show the syntheses of one line of Tb and Eu in Figure 6. Our S/N is good enough that the quality of our spectrum is not the problem. The gf-values and HFS and IS constants for these two species are based on laboratory studies. The line parameters are either the same as or very similar to the values used by Sneden et al. (1996, 2002), Hill et al. (2002) and Cowan et al. (2002) in their studies of extremely r-process-rich stars. Therefore, while it is possible that our knowledge of the atomic parameters for these lines is in error, such a revision would destroy the excellent agreement between the abundances in metal-poor r-process-rich stars and r_{ss}. We used the partition functions for Eu and Tb from the 2002 release of MOOG[4]. We have not included any corrections due to NLTE effects on the strong lines of EuII, but the work of Gehren et al. (2001) shows that this should be on the order of only 0.10 dex. HFS affects ^{151}Eu more than ^{153}Eu, so if the isotopic ratio was different than the 50-50 split seen in the solar system and predicted for the s-process (Arlandini et al. 1999), the Eu abundance could be too high. However, even assuming that all the Eu is in ^{151}Eu reduces the Eu abundance by only 0.05 dex. We have focused on Eu because we have HFS and IS information for its lines. Er is also high relative to s-process models, but we could not find information on the IS for our lines. Our largest Er EW is 64.4 mÅ, and we see no trend of increasing abundance with increasing EW. So we believe our Er abundance is accurate, but would like the HFS and IS data to confirm this. Eu/Ho and Eu/Dy in CS 31062-050 are also higher than predicted by the s-process models. Like Eu and Tb, Ho (93%) and Dy (85%) are mostly produced by the r-process in the solar system and therefore a match cannot be made to the observed ratios by adjusting contributions from s_{ss} and r_{ss}.

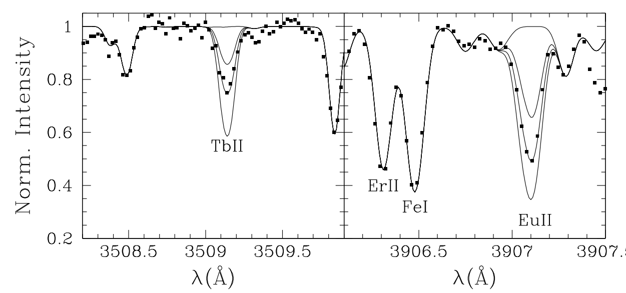

FIG. 6.— Spectral synthesis of a line of (left) Tb II and (right) Eu II. The solid squares are the data. The solid lines represent, in order of increasing strength and relative to our adopted log $\epsilon = -\infty$, −0.3 dex, 0.0 dex, and +0.3 dex.

Finally, we note that this study is not the only one to find ratios that cannot be explained by an s+r scenario. The Eu/Dy

[4]ftp verdi.as.utexas.edu

ratios for CS 22948-027 and CS 29497-034 in Hill et al. (2000) are so high (0.74 and 1.32, respectively) that they cannot be explained by a pure r-process (Eu/Dy=0.174), much less a pure s-process (Eu/Dy=0.097) or any combination therefore. Unfortunately, the Dy abundances in these two stars are based on only one line, so this conclusion is not as robust as the Eu/Tb ratio in CS 31062-050. Qian & Wasserburg (2003) point out that the abundance of Gd in HE 2148-1247 was too high to be fit by their best-fit single combination of s_{ss} and r_{ss}.

5.3. *The s-process and high Eu*

The results discussed in the previous sections are most economically explained by an s-process that produces more Eu than currently expected. Are there conditions in which an s-process produce such a high Eu/La ratio? To check this possibility, we looked at the s-process calculations of Malaney (1987a). These are parametric calculations, rather than calculations of the s-process in a specific AGB star. Because we wish to see if slow neutron-capture under any conditions will work, these are appropriate. Malaney (1987a) calculated abundances from Fe to Tl for a range of mean neutron exposures (τ_0) for two different neutron densities: $N_n = 10^8$ and $N_n = 10^{12}$. His calculations are for a solar metallicity number of seeds, so we would not expect his models to show the correct [ls/hs] metallicity dependence. One of his models, τ_0=0.05, $N_n = 10^{12}$, was a good match to the La/Eu ratio (Figure 7) and gives a reasonable match to our measured abundance pattern from La to Hf. Tb is a notable mismatch, and this neutron density is much higher than expected for the s-process conditions in an AGB star (Busso et al. 1999) in current models. In fact, Aoki et al. (2003) derived constraints on the neutron density and the temperature in CS 31062-050 by using isotopes of Eu that are sensitive to the branching point at ^{151}Sm. They measure a ^{151}Eu fraction of 0.55, higher than the solar value of 0.48, which indicates a neutron density of N_n=10^7-10^9. However, they make no predictions for the absolute Eu abundance in CS 31062-050 in that paper. In addition to variations in physical conditions between AGB stars, the details of s-process branchings in the Eu region are still subject to theory and laboratory-based revisions. For example Best et al. (2001) report new (n,γ) cross sections for ^{152,154}Sm, ^{151,153}Eu and ^{164,170}Sm based on laboratory measurements irradiating Sm, Eu and Er samples with neutrons with a quasistellar energy spectrum. Differences with previous measurements are in some cases as large as 50%, although there is a clear convergence with measurements by different groups since the 1990s show agreement at the 20% level. These authors also point out the uncertainties in the "stellar enhancement" corrections required to account for cross section and β-decay rate differences between laboratory and stellar interior conditions (due to the populations of low-lying excited states in many of the important nuclei). In the end, a successful model will need to fit both the Eu abundance and the Eu isotope fractions to explain the origin of Eu in this star using appropriate cross sections and physical conditions.

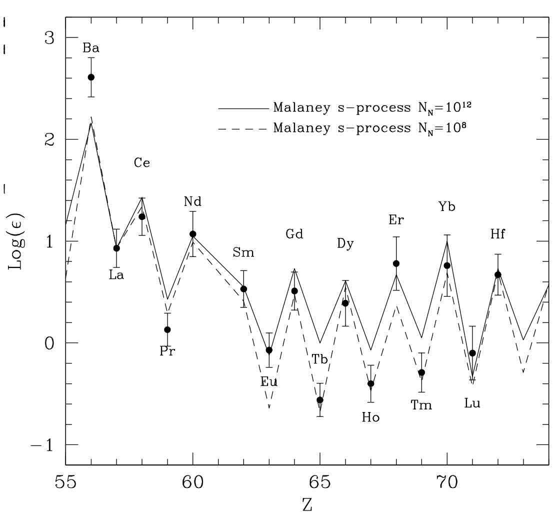

FIG. 7.— Comparison of the abundances for CS 31062-050 (solid circles) and a parametric s-process calculation of Malaney (1987a) with τ_0 and $N_n = 10^{12}$ and $N_n = 10^8$. The differences between the two neutron densities is a result of the nuclear flow passing through more neutron-rich nuclei if possible. These nuclei that have smaller neutron-capture cross-sections, thus altering the relative ratios of the elements (Malaney 1987b).

6. SUMMARY

We have determined the abundances of 20 neutron-capture elements in CS 31062-050. This is a C-rich star with several ratios of neutron-rich elements that match models of the metal-poor s-process. However, several well-measured heavy element ratios, most notably Eu/La, are inconsistent with any s-process predictions and the two ratios Eu/Tb and Eu/Dy cannot be explained by any combination of any s-process predictions and r-process predictions. High Eu/La (in the context of the s-process) has been seen before in CH stars leading some authors to suggest CH stars that are both s- and r-process-element rich. For CS 31062-050, our upper limit to the Th abundance argues against the r-process as the complete explanation, at least in this star. The Eu/Tb and Eu/Dy ratios suggests that our understanding of the s- or r-process yields are incomplete for at least some of these elements. An s-process that produces variable amounts of Eu in excess of the current models could eliminate the most glaring differences between observations and models.

Data presented herein were obtained at the W.M. Keck Observatory, which is operated as a scientific partnership among the California Institute of Technology, the University of California, and the National Aeronautics and Space Administration. The Observatory was made possible by the generous financial support of the W.M. Keck Foundation. Many thanks to Roberto Gallino for sharing the results of the s-process predictions in advance of publication and for many helpful insights on the workings of the s-process. We would also like to thank Sara Lucatello, Falk Herwig, and Jim Hesser for their comments on drafts of this paper. We gratefully acknowledge support from National Science Foundation grant AST-0098617.

APPENDIX

Atomic Parameters, Oscillator Strengths and Linelists

Copper: The usual Cu lines at λ5105Å and λ5782Å were undetectable, but we were able to measure the resonance lines at λ3273Å and λ3247Å. Because of the HFS and IS of these lines, we synthesized the regions. There are two isotopes of copper, ^{57}Cu and ^{59}Cu, both affected by HFS. The HFS and IS information was taken from Hermann et al. (1993), and the ratio of the isotopes seen in the solar system was used. Unfortunately, the S/N in this region is $\sim$ 25, even after co-adding the spectra from overlapping orders. Using the formula in Fulbright & Johnson (2003) to calculate the expected EW errors, we find that we need to include a σ = 0.20 dex in log ϵ to account for the observational errors.

Yttrium: The gf-values are from Hannaford et al. (1982). Y has one stable isotope, ^{89}Y, and it has HFS. However, Johnson & Bolte (2001) investigated the effect of including HFS on the measurement of the Y abundance in metal-poor stars, and found $<$ 0.01 dex effect. Therefore, HFS has not been included in this study either.

Zirconium: The gf-values for this element come from Bieḿont et al. (1981).

Barium: We originally measured the abundance of Ba using a set of strong lines (λ4554.0Å, λ5853.7Å, and λ6496.9Å) that we have used in previous studies. The gf-values and HFS information are from McWilliam (1998), and we used the isotope ratios produced by the s-process from Arlandini et al. (1999). The abundance from these three lines was log ϵ = 2.61, in disagreement with the results of A02 for the same star (log ϵ = 2.21). This discrepancy cannot be explained by the difference in model atmospheres. A02 used two different lines, λ4130 and λ4166. When we used these two lines, we derived a value of logϵ =2.46. This is an important point. With our high Ba value, Eu/Ba agrees with the s_{ss}. Our use of strong lines, much more sensitive to ξ, could be part of the problem. NLTE effects on the Ba II lines could also be important. However, we cannot rule out the possibility that the Ba abundance in this star is high. Our quoted error includes the contributions of EW errors and atmosphere parameters errors, but not systematic NLTE effects.

Lanthanum: Lanthanum has only one stable isotope, but HFS is important. We adopt both the gf-values and the HFS constants from the laboratory study of Lawler, Bonvallet, & Sneden (2001).

Cerium: Ce II has only two isotopes, ^{140}Ce and ^{142}Ce, that have a $>$1% contribution to the solar-system abundance. While our Ce II lines are weak, when we derived abundances assuming lines without splitting, the stronger lines gave higher abundances, which may indicate that IS cannot be ignored. We eliminated all lines with EW$>$40mÅ. Doing this brought the average Ce abundance down by 0.03 dex. We also tried including the approximate IS scheme of Aoki et al. (2001), where the ^{142}Ce line is shifted 0.11Å relative to the ^{140}Ce line. We used the solar system ratios for the relative abundances of the two Ce isotopes. This resulted in a change of 0.01 dex in the average abundance. The gf-values for this element are from Palmeri et al. (2000).

Praseodymium: New laboratory measurements of gf-values are available for Scholl et al. (2002). HFS constants are available for all ten lines we measured. The values of Li et al. (2000) or Rivest et al. (2002) were used if measured; otherwise the values from Ginibre (1989) were used.

Neodymium: Our first choice for gf-values for Nd were derived using lifetimes from Scholl et al. (2002) or Pinciuc et al. (2001) and branching ratios from Maier & Whaling (1977). Otherwise our gf-values were adopted from KUR95. There are seven stable Nd isotopes, and we used the solar system isotopic abundances. While two of the isotopes have odd Z, we neglect HFS for our lines since we could not find HFS constants in the literature. We adopted IS from Nakhate, Afzal, & Ahmad (1997) if available or from Blaise et al. (1984). All but four of our transitions were covered. The splitting ratios were taken from Aoki et al. (2001).

Samarium: The gf-values are either taken directly from Biémont et al. (1989) or were computed using the branching ratios of Saffman & Whaling (1979) and the lifetimes of Biémont et al. (1989) or Vogel et al. (1988). We have IS information for most lines. The IS are from Villemoes et al. (1995) and Rao et al. (1990). The splittings ratios are given in Villemoes et al. (1995), and we used the solar system isotope ratios. Two Sm isotopes, ^{147}Sm and ^{149}Sm have HFS. We were unable to find HFS constants for our transitions, but these two isotopes contribute $<$ 30% to the solar system abundances.

Europium: The five lines we analyzed have gf-values, HFS constants, IS constants in Lawler et al. (2001b). ^{151}Eu and ^{153}Eu are produced in approximately equal proportions in the r-process and the s-process (Arlandini et al. 1999) so we have adopted a 50:50 split for our analysis.

Gadolinium: Our first choice for gf-values was Bergstrom et al. (1988). We added additional oscillator strengths from the compilation of Corliss & Bozman (1962), following Bergstrom et al.'s suggestion that the log gf values of CB should be increased by 0.11 dex. We found that the IS of the seven stable isotopes of Gd had an effect on the derived abundances if the EW was too large. Since we could not find IS for all of the transitions, we use only those lines with EW $<$ 35mÅ or with IS information. This information was gathered from Brix et al.(1952), Ahmad, Saksena, & Venugopalan (1976), Ahmad, Venugopalan, & Saksena (1979), and Venugopalan, Afzal, & Ahmad (1998). The isotopic splitting ratios are from Kopfermann, Kruger, & Steudel (1957).

Terbium: There is only one stable isotope of Tb, ^{159}Tb. We adopted gf-values from Lawler et al. (2001a) and HFS constants from Lawler, Wyart, & Blaise (2001).

Dysprosium: There are seven stable isotopes of Dy, and all are made in the s-process. Two of the isotopes have odd Z and so have hyperfine splitting, but we couldn't find information on our transitions. We did find information on IS for most of our transitions in Aufmuth (1978). We used the solar system isotope ratios. The gf-values are from Wickliffe, Lawler and Nave (2000)

Holmium: There is only one stable isotope of Ho, ^{165}Ho, but HFS is important. For λ4045, we use the Sneden et al. (1996) linelist, with their HFS and gf-value. For λ3398 and λ3416, we adopt HFS constants from Worm, Shi, & Poulsen (1990). The gf-value of λ3398 comes from Gorshkov & Komarovskii (1979), while the gf-valueof λ3416 was taken from the Kurucz linelist.

Erbium: We confine our analysis to lines with oscillator

strengths from Musiol & Labuz (1983). We were unable to find IS or HFS information for the observed transitions in the literature.

Thulium: Wickliffe & Lawler (1997) have recently published high-quality gf-values for Tm transitions, including the four included in this study. No HFS information was available, but all lines had EW $<$ 20 mÅ, so our abundance analysis should be accurate.

Ytterbium: The gf-value for the one line of Yb we could use is from Pinnington, Rieger, & Kernahan (1997). The IS and HFS information is from Mårtensson-Pendrill, Gough, & Hannaford (1994). The isotope ratios are the predicted s-process ones from Arlandini et al. (1999).

Hafnium: There are five isotopes of Hf; two of those have hyperfine splitting. We could only find information for the strongest line (3399.8Å) out of the eleven we used (Zhao et al. 1997). The HFS is considerably larger than the isotopic splitting. The use of the IS (with solar system ratios) and HFS reduces the abundance derived from the 3399.8Å by 0.64 dex. While the other lines have no information, they are weaker (EW $<$ 35mÅ), and their average abundance is equal to that derived from the 3399Å.

Lead: We adopt the line lists from Johnson & Bolte (2002a).

REFERENCES

Ahmad, S. A., Saksena, G. D., & Venugopalan, A. 1976, Physica B&C, 81, 366
Ahmad, S. A., Venugopalan, A., & Saksena, G. D. 1979, Spectrochimica Acta, 34B, 221
Aoki, W., Norris, J. E., Ryan, S. G., Beers, T. C., & Ando, H. 2000, ApJ, 536, L97
Aoki, W., Ryan, S. G., Iwamoto, N., Beers, T. C., Norris, J. E., Ando, H., Kajino, T., Mathews, G. J., & Fujimoto, M. Y. 2003, ApJ, 592, L67
Aoki, W., Ryan, S. G., Norris, J. E., Beers, T. C., Ando, H., Iwamoto, N., Kajino, T., Mathews, G. J., & Fujimoto, M. Y. 2001, ApJ, 561, 346
Aoki, W., Ryan, S. G., Norris, J. E., Beers, T. C., Ando, H., & Tsangarides, S. 2002, ApJ, 580, 1149
Arlandini, C. Käppeler, F., Wisshak, K., Gallino, R., Lugaro, M., Busso, M., & Straniero, O. 1999, ApJ, 525, 886
Aufmuth, P. 1978, Z. Physik A, 286, 235
Bergström, Biémont, E., Lundberg, H., & Persson, A. 1988, A&A, 192, 335
Best, J., Stoll, H., Arlandini, C., Jang, S., Käppeler, F., Wisshak, K., Mengoni, R., Reffo, G., & Rauscher, T. 2001, Phys Rev C., 64, 015801-1
Biémont, E., Grevesse, N., Hannaford, P., & Lowe, R. M. 1981, ApJ, 248, 867
Biémont, E., Grevesse, N., Hannaford, P., & Lowe, R. M. 1989, A&A 222, 307
Biémont, E., Grevesse, N., Kwiatkowski, M., Zimmermann, P. 1982, A&A, 108, 127
Blaise, J., Wyart, J.-F., Djerad, M. T., & Ahmed, Z. B. 1984, Phys. Scr. 29, 119
Burbidge, E. M., Burbidge, G. R., Fowler, W. A., & Hoyle, F. 1957, Rev. Mod. Phys., 29, 547
Busso, M., Gallino, R., Lambert, D. L., Travaglio, C., & Smith, V. V. 2001, ApJ, 557, 802
Cayrel, R., et al.. 2001, Nature, 409, 691
Clayton, D. D. & Rassbach, M. E. 1967, 148, 69
Cohen, J. G., Christlieb, N., Qian, Y.-Z., & Wasserburg, G. J. 2003, ApJ, 588, 1082
Corliss, C. H., & Bozman, W. R. 1962, Experimental Transition Probabilities for Spectral Lines of Seventy Elements (NBS Monograph 32) (Washington: GPO)
Cowan, J. J., Pfeiffer, B., Kratz, K.-L., Thielemann, F.-K., Sneden, C., Burles, S., Tytler, D., & Beers, T. C. 1999, ApJ, 521, 194
Cowan, J. J. et al. 2002, ApJ, 572, 861
Den Hartog, E. A., Curry, J. J., Wickliffe, M. E., & Lawler, J. E. 1998, Sol. Phys. 178, 239
Fulbright, J. P., & Johnson, J. A. 2003, ApJ, in press (astro-ph/0307063)
Gallino, R., Arlandini, C., Busso, M., Lugaro, M., Travaglio, C., Straniero, O., Chieffi, A., & Limongi, M. 1998, ApJ, 497, 388
Gilroy, K. K., Sneden, C., Pilachowski, C., & Cowan, J. J. 1988, ApJ, 327, 298
Ginibre, A. 1989, Phy. Scr. 39, 694
Goriely, S. & Mowlavi, N. 2000, A&A, 362, 599
Gorshkov, V. N. & Komarovskii, V. A., 1979, Opt. Spectrosk. 47, 631
Grevesse, N., Noels, A., & Sauval, A. 1996, in ASP Conf. Ser. 99, Cosmic Abundances, ed. S. Holt & G. Sonneborn (San Francisco: ASP), 117
Hannaford, P., Lowe, R. M., Grevesse, N., Biémont, E., & Whaling, W. 1982, ApJ, 261, 736
Hermann, G., Lasnitschka, G., Schwabe, C., & Spengler, D. 1993, Spectrochim. Acta B, 48B, 1259
Hill, V., Barbuy, B., Spite, M., Spite, F., Cayrel, R., Plez, B., Beers, T. C., Nordström, B., & Nissen, P. E. 2000, A&A, 353, 557 137, 341
Hill, V. et al. 2002, A&A, 387, 560
Johnson, J. A. 2002, ApJS, 139, 219
Johnson, J. A. & Bolte, M. 2001, ApJ, 554, 888
Johnson, J. A. & Bolte, M. 2002a, ApJ, 579, L87
Johnson, J. A. & Bolte, M. 2002b, ApJ, 579, 616
Käppeler, F., Beer, H., & Wisshak, K. 1989, Rep. Prog. Phys. 52, 945
Kopfermann, H., Krüger, L., & Steudel, A. 1957, Ann. Phys. 20, 258
Kurucz, R. L., & Bell, B. 1995, 1995 Atomic Line Data, Kurucz CD-Rom #23 (Cambridge, MA: SAO)
Lattimer, J. M., & Schramm, D. N. 1974, ApJ, 192, 145
Lawler, J. E., Bonvallet, G., & Sneden, C. 2001, ApJ, 556, 452
Lawler, J. E., Wickliffe, M. E., Cowley, C. R., E. A., & Sneden, C. 2001a, ApJS, 137, 341
Lawler, J. E., Wickliffe, M. E., den Hartog, E. A., & Sneden, C. 2001b, ApJ, 563, 1075
Lawler, J. E., Wyart, J.-F., & Blaise, J. 2001c, ApJS, 137, 351
Li, M., Ma, H., Chen M. Lu, F., Tang, J., & Yang, F. 2000, Phy. Rev. A, 62, 052504
Lucatello, S., Gratton, R., Cohen, J. G., Beers, T. C., Christlieb, N., Carretta, E., & Ramírez, S. 2003, AJ, 125, 875
Maier, R. S. & Whaling, W. 1977, JQSRT, 18, 501
Malaney, R. A. 1987a, ApJ, 321, 832
Malaney, R. A. 1987b, ApS&S, 137, 251
Mårtensson-Pendrill, A.-M., Gough, D. S., & Hannaford, P. 1994, Phy. Rev. A 49, 3351
Mashonkina, L., & Gehren, T. 2001, A&A, 376, 232
Matteucci, F., Raiteri, C. M., Busso, M., Gallino, R., & Gratton, R. 1993, A&A, 272, 421
McClure, R. D. 1984, ApJ, 280, L31
McClure, R. D. & Woodsworth, A. W. 1990, ApJ, 352, 709
McWilliam, A. 1998, AJ, 115, 1640
McWilliam, A., Preston, G. W., Sneden, G., & Searle, L. 1995, AJ, 109, 2757
Moity, J. 1983, A&AS, 52, 37
Moore, C. E., Minnaert, M. G. J., & Houtgast, J. 1966, The Solar Spectrum, 2935Å to 8770Å (NBS Monog. 61, Washington DC: NBS)
Musiol, K. & Labuz, S. 1983, Phys. Scr. 27, 422
Nakhate, S. G., Afzal, S. M., & Ahmad, S. A. 1997, Z. Phy. A.
Nilsson, H., Zhang, Z. G., Lundberg, H., Johansson, S., & Nordström, B. 2002, A&A. 382. 368
Norris, J. E., Ryan, S. G., & Beers, T. C. 1997, ApJ, 489, L169
Palmeri, P., Quinet, P., Wyart, J.-F., & Biemont, E. 2000, Physica Scripta, 61, 323
Pinciuc, C. M., Rivest, R. C., Izawa, M. R., Holt, R. A., Rosner, S. D., & Scholl, T. J. 2001, Can. J. Phys. 79, 1159
Pinnington, E. H., Rieger, G., & Kernahan, J. A. 1997, Phy. Rev. A, 56, 2421
Preston, G. W., & Sneden, C. 2001, AJ, 122, 1545
Primas, F., Brugamyer, E., Sneden, C., King, J. R., Beers, T. C., Boesgaard, A.M., & Deliyannis, C. P. 2000, in The First Stars, ed. A. Weiss, T. G. Abel, & V. Hill (Springer), 51
Qian, Y.-Z. & Wasserburg, G. J. 2003, ApJ, 588, 1099
Rao, P. M., Ahmad, S. A., Venugopalan, A., & Saksena, G. D. 1990, Z. Phys. D. 15, 211
Rivest, R.C., Izawa, M. R., Rosner, S. D., Scholl, T. J., Wu, G., & Holt, R. A. 2002, Can. J. Phys. 80, 557
Rosswog, S., Davies, M. B., Thielemann, F.-K., & Piran, T. 2000, A&A, 360, 171
Saffman, L. & Whaling, W. 1979, JQRST, 21, 93
Scholl, T. J., Holt, R. A., Masterman, D., Rivest, R. C., Rosner, S. D., & Sharikova, A. 2002, Can. J. Phys. 80, 713
Sheinis, A. I., Bolte, M., Epps, H. W., Kibrick, R. I., Miller, J. S., Radovan, M. V., Bigelow, B. C., & Sutin, B. M. 2002, PASP, 114, 851
Sneden, C. 1973, Ph.D. thesis
Sneden. C., Cowan, J. J., Ivans, I. I., Fuller, G. M., Burles, C., Burles, T. C., & Lawler, J. E. 2000, ApJ, 533, L139
Sneden, C., Cowan, J. J., Lawler, J. E., Burles, S., Beers, T. C., & Fuller, G. M. 2002, ApJ, 566, L25
Sneden, C., Gratton, R. G., & Crocker, D. A. 1991, A&A, 246, 354
Sneden, C., McWilliam, A., Preston, G. W., Cowan, J J., Burris, D. L., & Armosky, B. J. 1996, ApJ, 467, 819.
Sneden, C., & Parthasarathy, M. 1983, ApJ, 267, 757
Truran, J. W., Cowan, J. J., Pilachowski, C. A., & Sneden, C. 2002, PASP, 114, 1293

Van Eck, S., Goriely, S., Jorissen, A., & Plez, B. 2001, Nature, 412, 793
Van Eck, S., Goriely, S., Jorissen, A., & Plez, B. 2003, A&A, 404, 291
Vanture, A. D., Wallerstein, G., Brown, J. A., & Bazan, G. 1991, ApJ, 381, 278
Venugopalan, A., Afzal, S. M., & Ahmad, S. A. 1998, Spectro. Acta B, 53, 633
Villemoes, P., Wang, M., Arnesen, A., Weiler, C., & Wännström, A. 1995, Phy. Rev. A, 51, 2838
Vogel, O., Edvardsson, B., Wännström, A., Arnesen, A., & Hallin, R. 1988, Phy. Scr. 38, 567
Vogt, S. S., et al. 1994, Proc. SPIE, 2198, 362
Westin, J., Sneden, C., Gustafsson, B., & Cowan, J. J. 2000, ApJ, 530, 783
Wickliffe, M. E. & Lawler, J. E. 1997, J. Opt. Soci. Am. B, 14, 737
Wickliffe, M. E., Lawler, J. E., & Nave, G. 2000, JQRST, 66, 363
Woosley, S. E. & Hoffman, R. D., 1992, ApJ. 395, 202
Woosley, S. E., Wilson, J. R., Mathews, G. J., Hoffman, R. D., & Meyer, B. S. 1994, ApJ, 433, 229
Worm, T., Shi, P., & Poulsen, O. 1990, Phys. Scr. 42, 569
Zhao, W. Z., Buchinger, F., Crawford, J. E., Fedrigo, S., Gulick, S., Lee, J. K. P., Constantinescu, O., Hussonnois, M., & Pinard, J. 1997, Hyperfine Interactions, 108, 483

TABLE 1
EQUIVALENT WIDTHS

λ Å	E.P. (eV)	log gf	Method	EW mÅ	HFS, IS?	log ϵ
			MgI			
4703.00	4.34	–0.523	EW	73.8		6.01
			CaI			
4318.65	1.90	–0.208	EW	43.5		4.36
5261.71	2.52	–0.580	EW	12.7		4.50
			TiI			
3653.50	0.05	0.280	EW	34.8		2.52
3729.81	0.00	–0.290	EW	38.0		3.10
3741.06	0.02	–0.150	EW	41.1		3.05
3752.86	0.05	0.040	EW	23.1		2.45
4533.24	0.85	0.540	EW	23.8		2.71
4534.78	0.84	0.340	EW	22.1		2.86
4617.27	1.75	0.450	EW	7.5		3.11
4981.73	0.85	0.560	EW	39.4		3.02
5210.39	0.05	–0.820	EW	13.1		2.85
			TiII			
4450.48	1.08	–1.510	EW	39.5		2.72
4468.49	1.13	–0.600	EW	80.6		2.91
4501.27	1.12	–0.760	EW	74.6		2.89
4657.20	1.24	–2.320	EW	12.1		2.94
			VII			
3545.19	1.10	–0.259	EW	26.5		1.30
3592.02	1.10	–0.263	EW	37.5		1.58
			CrI			
4600.76	1.00	–1.260	EW	13.4		3.57
4626.18	0.97	–1.320	EW	6.0		3.20
4646.17	1.03	–0.720	EW	21.2		3.31
			MnI			
3823.51	2.14	–0.513	EW	13.8	HFS	2.86
4030.74	0.00	–1.037	EW	89.0	HFS	2.64
4033.09	0.00	–1.291	EW	77.0	HFS	2.57
4754.04	2.28	–0.677	EW	6.9	HFS	2.69
			FeI			
3617.78	3.02	–0.050	EW	43.3		5.07
3709.25	0.92	–0.610	EW	99.0		5.04
3715.91	2.28	–1.530	EW	20.9		5.08
3760.05	2.40	–0.810	EW	38.2		4.93
3767.19	1.01	–0.350	EW	96.4		4.79
3787.88	1.01	–0.820	EW	86.4		4.97
3790.10	0.99	–1.720	EW	56.3		4.86
3856.37	0.05	–1.250	EW	116.0		5.11
3899.71	0.09	–1.490	EW	95.4		4.92
3906.48	0.11	–2.200	EW	81.5		5.22
3916.74	3.24	–0.560	EW	20.9		5.06
3917.18	0.99	–2.150	EW	55.0		5.22
3922.91	0.05	–1.610	EW	97.6		5.05
3949.96	2.17	–1.250	EW	34.7		5.02
4114.45	2.83	–1.300	EW	13.0		5.10
4147.68	1.49	–2.060	EW	41.7		5.25
4156.81	2.83	–0.810	EW	38.7		5.32
4187.04	2.45	–0.510	EW	57.3		5.10
4202.03	1.49	–0.670	EW	87.3		5.19
4216.19	0.00	–3.320	EW	43.8		4.99
4222.22	2.45	–0.930	EW	38.2		5.03
4233.61	2.48	–0.560	EW	51.3		5.01
4250.13	2.47	–0.370	EW	67.2		5.25
4494.57	2.20	–1.100	EW	46.6		5.11
4531.15	1.49	–2.110	EW	36.7		5.14
4871.32	2.85	–0.360	EW	53.3		5.17
4872.14	2.87	–0.570	EW	39.8		5.08
4891.49	2.84	–0.110	EW	67.7		5.29
4903.31	2.87	–0.930	EW	23.9		5.06
4920.50	2.82	0.070	EW	66.0		5.04
4994.13	0.92	–3.040	EW	25.1		5.15
5006.12	2.83	–0.660	EW	41.9		5.17
5041.07	0.95	–3.090	EW	17.5		5.02
5049.82	2.28	–1.340	EW	44.0		5.32
5051.64	0.92	–2.760	EW	31.7		5.03
5166.29	0.00	–4.160	EW	16.7		5.06
5171.60	1.49	–1.750	EW	54.8		5.14
5192.34	2.99	–0.420	EW	43.3		5.11
5194.94	1.56	–2.050	EW	36.9		5.10
5198.71	2.22	–2.090	EW	9.2		5.01

TABLE 1
EQUIVALENT WIDTHS

λ Å	E.P. (eV)	log gf	Method	EW mÅ	HFS, IS?	log ϵ
5216.28	1.61	−2.110	EW	25.9		4.95
5217.39	3.21	−1.070	EW	12.9		5.18
5232.94	2.94	−0.100	EW	57.3		5.07
5242.49	3.62	−0.970	EW	5.0		5.04
5266.56	2.99	−0.380	EW	37.1		4.93
5269.54	0.86	−1.330	EW	94.6		5.18
			FeII			
4491.40	2.86	−2.710	EW	14.2		5.03
4508.29	2.86	−2.330	EW	26.0		5.00
4520.23	2.81	−2.600	EW	26.9		5.24
4555.89	2.83	−2.390	EW	21.3		4.90
4582.84	2.84	−3.100	EW	10.1		5.21
4583.84	2.81	−1.920	EW	49.4		5.08
4629.34	2.81	−2.370	EW	31.6		5.12
5018.45	2.89	−1.220	EW	80.5		5.27
5197.56	3.23	−2.100	EW	19.8		4.94
5234.62	3.22	−2.230	EW	24.7		5.19
			CoI			
4121.30	0.92	−0.993	EW	37.4	HFS	2.60
			NiI			
3500.85	0.17	−1.294	EW	56.8		3.50
3515.05	0.11	−0.266	EW	94.6		3.67
3519.77	0.28	−1.422	EW	53.6		3.62
3524.54	0.03	−0.007	EW	105.5		3.55
3571.87	0.17	−1.154	EW	76.5		4.05
3597.71	0.21	−1.115	EW	66.0		3.67
3602.28	0.17	−2.192	EW	31.3		3.60
3612.74	0.28	−1.423	EW	58.7		3.77
3619.39	0.42	0.020	EW	87.9		3.49
3664.10	0.28	−2.130	EW	35.3		3.67
3858.30	0.42	−0.951	EW	77.2		3.87
			CuI			
3247.58	0.00	−0.421	syn	58.1	HFS,IS	0.59
3273.98	0.00	−0.864	syn	54.0	HFS,IS	0.79
			ZnI			
4810.55	4.08	−0.170	EW	8.8		2.32
			YII			
3549.01	0.13	−0.280	EW	38.8		0.23
3584.52	0.10	−0.410	syn	39.4		0.34
3600.74	0.18	0.280	syn	53.2		0.19
3601.91	0.10	−0.180	syn	45.5		0.29
3611.04	0.13	0.010	syn	45.9		0.14
3628.70	0.13	−0.710	syn	26.3		0.29
3710.29	0.18	0.460	syn	64.9		0.29
3774.34	0.13	0.210	syn	57.5		0.19
3950.36	0.10	−0.490	syn	38.5		0.24
4854.87	0.99	−0.380	EW	18.1		0.41
4883.69	1.08	0.070	EW	32.2		0.43
4900.11	1.03	−0.090	syn	28.0		0.44
5087.42	1.08	−0.170	syn	23.5		0.44
5200.41	0.99	−0.570	EW	10.1		0.26
			ZrII			
3458.94	0.96	−0.520	syn	10.3		0.91
3479.39	0.71	0.170	syn	36.0		0.81
3505.67	0.16	−0.360	EW	44.1		1.00
3551.96	0.09	−0.310	syn	51.3		1.11
4050.33	0.71	−1.000	EW	9.1		0.93
4208.98	0.71	−0.460	EW	35.0		1.19
4258.05	0.56	−1.130	syn	15.7		1.16
4443.00	1.49	−0.330	syn	10.6		1.11
4496.97	0.71	−0.810	syn	23.4		1.21
			PdI			
3404.58	0.81	0.320	syn	9.2		0.17
			LaII			
3628.82	0.13	−1.763	syn	21.5	HFS	0.84
3713.57	0.17	−1.372	syn	40.2	HFS	0.74
3794.77	0.24	−0.473	syn	56.5	HFS	0.60
3929.24	0.17	−0.962	syn	81.6	HFS	1.04
3988.56	0.40	−0.475	EW	129.1	HFS	0.89
3995.78	0.17	−0.706	EW	94.1	HFS	0.96
4086.71	0.00	−0.696	syn	71.6	HFS	0.90
4123.22	0.32	−0.482	syn	75.4	HFS	0.95

TABLE 1
EQUIVALENT WIDTHS

λ Å	E.P. (eV)	log gf	Method	EW mÅ	HFS, IS?	log ϵ
4322.54	0.17	−1.532	syn	52.8	HFS	0.99
4526.10	0.77	−1.222	EW	25.8	HFS	0.92
4558.46	0.32	−1.572	syn	27.3	HFS	0.84
4574.95	0.17	−1.706	EW	39.6	HFS	0.88
4580.04	0.71	−1.390	syn	12.3	HFS	0.84
4613.37	0.71	−1.283	syn	29.0	HFS	1.09
4645.31	0.13	−2.455	syn	9.0	HFS	0.84
4662.52	0.00	−1.763	syn	32.7	HFS	0.89
4716.41	0.77	−1.733	EW	8.3	HFS	0.87
4728.45	0.17	−1.982	syn	28.0	HFS	0.99
4740.28	0.13	−1.652	EW	40.6	HFS	1.07
4804.01	0.23	−2.084	EW	28.4	HFS	1.17
4808.99	0.23	−1.780	EW	20.6	HFS	0.92
4824.03	0.65	−1.250	syn	25.2	HFS	0.99
4840.01	0.32	−2.416	EW	10.3	HFS	1.10
4970.39	0.32	−1.683	syn	26.0	HFS	0.99
4986.86	0.17	−1.823	syn	25.7	HFS	0.84
			CeII			
3534.06	0.52	−0.210		23.0		1.20
3539.08	0.32	−0.500		28.0		1.43
3577.47	0.47	0.080		34.8		1.21
3653.66	0.47	−0.190		19.3		0.93
3655.85	0.32	−0.150		29.5		1.04
3659.23	0.17	−0.790		21.4		1.28
3709.95	0.12	−0.320		36.6		1.19
3764.11	0.36	−0.220		35.0		1.28
3838.54	0.33	−0.100		42.5		1.33
3896.78	0.56	−0.410		18.5		1.18
3919.82	0.70	−0.220		26.7		1.38
3923.11	0.56	−0.630		24.5		1.58
3924.65	0.56	−0.280		19.5		1.08
3940.36	0.32	−0.380		33.9		1.34
3942.75	0.86	0.670		40.3		1.03
3960.92	0.32	−0.460		26.2		1.20
4003.77	0.93	0.200		24.6		1.13
4031.34	0.32	−0.150		33.0		1.06
4042.59	0.50	0.110		41.7		1.23
4046.34	0.55	−0.710		26.6		1.69
4053.49	0.00	−0.800		29.8		1.28
4062.23	1.37	0.300		16.7		1.24
4068.83	0.70	−0.220		35.7		1.60
4073.49	0.48	0.180		44.4		1.21
4075.71	0.70	0.270		36.5		1.13
4083.23	0.70	0.190		39.1		1.29
4115.38	0.92	0.050		24.6		1.26
4118.15	0.70	0.140		37.5		1.29
4127.38	0.68	0.300		42.3		1.23
4137.65	0.52	0.390		55.1		1.38
4145.00	0.70	0.090		33.9		1.23
4148.92	1.09	−0.010		13.7		1.14
4165.60	0.91	0.480		42.0		1.28
4444.40	0.92	−0.110		21.4		1.29
4444.70	1.06	0.080		24.6		1.33
4460.23	0.48	0.270		58.0		1.48
4486.91	0.30	−0.330		41.0		1.36
4523.08	0.52	−0.080		50.4		1.61
4528.48	0.86	0.330		34.8		1.13
4539.78	0.33	−0.080		43.1		1.19
4560.97	0.68	−0.220		20.1		1.09
4565.86	1.09	−0.010		19.3		1.29
4593.94	0.70	0.070		49.8		1.63
4562.37	0.48	0.190		52.9		1.37
4628.16	0.52	0.150		47.6		1.28
4773.96	0.92	−0.330		11.7		1.13
4882.49	1.53	0.200		11.3		1.21
5044.03	1.21	−0.140		8.5		1.06
5187.46	1.21	0.080		19.3		1.27
5274.24	1.04	0.080		23.8		1.21

TABLE 1
EQUIVALENT WIDTHS

λ Å	E.P. (eV)	log gf	Method	EW mÅ	HFS, IS?	log ϵ
			PrII			
3964.88	0.05	–0.503	SYN	41.2	HFS	0.04
3965.33	0.20	–0.432	SYN	41.0	HFS	0.11
4044.75	0.00	–0.803	SYN	21.7	HFS	–0.01
4062.74	0.42	–0.148	SYN	43.6	HFS	0.09
4143.20	0.37	–0.098	SYN	67.0	HFS	0.19
4179.47	0.20	–0.248	SYN	74.9	HFS	0.24
5173.89	0.97	–0.179	SYN	12.1	HFS	–0.01
5219.03	0.80	–0.812	SYN	8.9	HFS	0.29
5220.10	0.80	–0.417	SYN	17.1	HFS	0.24
5259.72	0.63	–0.502	SYN	16.6	HFS	0.14
			NdII			
3713.70	0.74	0.080	SYN	21.5		0.75
3715.69	0.47	–0.190	SYN	27.2	IS	0.90
3780.40	0.47	–0.130	SYN	27.9	IS	0.84
3784.25	0.38	0.390	EW	50.7	IS	0.92
3900.23	0.47	0.340	SYN	45.2	IS	0.86
3941.51	0.06	–0.010	SYN	51.8	IS	0.96
3957.99	0.06	–0.650	SYN	35.2	IS	1.09
3973.25	0.63	0.210	EW	47.9	IS	1.19
3976.12	0.21	–1.200	SYN	13.4	IS	1.14
3976.84	0.00	–0.590	SYN	43.2	IS	1.18
3979.47	0.21	–0.280	SYN	49.5	IS	1.25
3992.59	1.41	0.160	SYN	17.5		1.20
4011.08	0.47	–0.830	EW	12.4		1.00
4012.23	0.63	0.780	SYN	74.1	IS	1.14
4012.70	0.00	–0.740	SYN	36.5	IS	1.15
4013.23	0.18	–1.150	EW	14.8		1.11
4018.82	0.06	–0.890	SYN	28.6	IS	1.15
4020.86	0.32	–0.270	SYN	45.3	IS	1.23
4021.33	0.32	0.230	SYN	44.2	IS	0.75
4021.75	0.18	–0.300	SYN	42.4	IS	1.05
4023.00	0.21	–0.200	SYN	47.0	IS	1.14
4043.59	0.32	–0.510	EW	24.3	IS	0.92
4051.14	0.38	0.090	EW	39.5	IS	0.80
4061.07	0.47	0.520	SYN	67.8	IS	1.14
4109.44	0.00	–0.810	SYN	25.1	IS	0.86
4113.83	0.18	–0.900	SYN	29.6	IS	1.29
4133.35	0.32	–0.510	SYN	32.8	IS	1.12
4156.07	0.18	0.180	EW	69.9	IS	1.17
4211.29	0.21	–0.720	SYN	30.0	IS	1.15
4446.37	0.21	–0.590	EW	46.5	IS	1.38
4451.55	0.38	0.110	SYN	61.4	IS	1.13
4451.98	0.00	–1.340	EW	26.6	IS	1.41
4567.60	0.21	–1.510	EW	9.3	IS	1.19
4579.32	0.74	–0.650	SYN	15.0	IS	1.15
4645.77	0.56	–0.750	EW	20.4	IS	1.22
5092.78	0.38	–0.610	EW	28.1	IS	1.04
5192.62	1.14	0.310	SYN	35.2	IS	1.10
5200.12	0.56	–0.490	EW	10.7	IS	0.56
5212.35	0.21	–0.870	EW	24.2	IS	1.02
			SmII			
3568.28	0.48	0.290	SYN	36.9	IS	0.42
3609.49	0.28	0.140	SYN	34.3	IS	0.41
3634.29	0.18	0.020	SYN	44.9		0.80
3706.75	0.48	–0.630	SYN	8.6		0.45
3718.88	0.38	–0.350	EW	22.8	IS	0.60
3896.97	0.04	–0.580	SYN	20.9		0.40
4244.70	0.28	–0.730	SYN	11.3	IS	0.40
4499.48	0.25	–1.010	EW	12.6	IS	0.68
4519.63	0.54	–0.430	SYN	19.5	IS	0.61
4523.90	0.43	–0.580	EW	21.1	IS	0.70
4577.69	0.25	–0.770	EW	16.6	IS	0.58
4815.81	0.18	–0.760	EW	13.9		0.37
			EuII			
3907.09	0.21	–0.374	SYN	72.0	HFS,IS	–0.10
3930.50	0.21	–0.326	SYN	87.8	HFS,IS	–0.10
4129.76	0.00	–0.401	SYN	115.0	HFS,IS	–0.12
4205.04	0.00	–0.386	SYN	106.3	HFS,IS	–0.10
4435.53	0.21	–0.696	SYN	78.2	HFS,IS	0.05

TABLE 1
EQUIVALENT WIDTHS

λ Å	E.P. (eV)	log gf	Method	EW mÅ	HFS, IS?	log ϵ
			GdII			
3331.40	0.00	–0.140	SYN	28.6		0.47
3392.50	0.08	–0.220	SYN	25.0		0.51
3418.70	0.00	–0.310	EW	23.2		0.45
3423.92	0.00	–0.410	SYN	20.6		0.46
3424.59	0.35	–0.170	SYN	19.3	IS	0.54
3439.21	0.38	0.150	EW	24.7	IS	0.42
3451.24	0.38	–0.050	SYN	18.2		0.42
3454.91	0.03	–0.590	SYN	18.8		0.61
3464.00	0.43	0.390	SYN	37.9	IS	0.54
3467.27	0.43	0.150	SYN	28.4	IS	0.58
3468.99	0.43	0.150	SYN	30.7		0.66
3473.22	0.03	–0.300	EW	32.4		0.74
3481.28	0.60	0.450	SYN	30.0		0.52
3481.80	0.49	0.230	SYN	24.7	IS	0.45
3549.40	0.24	0.310	EW	37.3	IS	0.45
3654.62	0.08	0.070	SYN	32.0		0.31
3699.74	0.35	–0.150	SYN	18.7		0.41
3719.53	0.49	0.120	SYN	15.4	IS	0.17
3916.51	0.60	0.170	SYN	28.6		0.61
4037.97	0.56	–0.230	SYN	17.4	IS	0.58
4063.38	0.99	0.470	SYN	24.0	IS	0.55
4085.56	0.73	0.070	EW	19.9	IS	0.57
4098.60	0.60	0.390	SYN	37.2	IS	0.60
4130.40	0.73	0.210	SYN	29.7	IS	0.68
			TbII			
3509.18	0.00	0.162	syn	29.60	HFS	–0.70
3568.55	0.00	–0.179	syn	12.60	HFS	–0.80
3702.81	0.13	–0.091	syn	14.20	HFS	–0.75
4005.43	0.13	–0.551	syn	5.10	HFS	–0.80
			DyII			
3407.80	0.00	0.180	syn	44.0	IS	0.39
3434.37	0.00	–0.450	EW	19.7	IS	0.21
3445.57	0.00	–0.150	EW	37.4	IS	0.46
3454.32	0.10	–0.140	syn	32.1		0.40
3460.97	0.00	–0.070	EW	35.8	IS	0.33
3523.98	0.54	0.420	syn	32.3	IS	0.28
3531.71	0.00	0.770	syn	60.4	IS	0.38
3534.96	0.10	–0.040	syn	32.7	IS	0.29
3536.02	0.54	0.530	EW	38.6	IS	0.37
3538.52	0.00	–0.020	EW	44.4	IS	0.53
3546.83	0.10	–0.550	syn	20.9	IS	0.44
3550.22	0.59	0.270	EW	30.6	IS	0.43
3563.15	0.10	–0.360	syn	25.7		0.40
3694.81	0.10	–0.110	syn	37.3	IS	0.39
3747.82	0.10	–0.810	syn	16.1		0.45
3757.37	0.10	–0.170	syn	35.8		0.40
3841.31	0.10	–0.780	syn	13.4		0.30
3983.65	0.54	–0.310	syn	16.7		0.40
3996.69	0.59	–0.260	syn	18.1		0.45
4077.97	0.10	–0.040	syn	42.4		0.40
			HoII			
3399.03	0.00	–0.496		62.5		–0.22
3416.37	0.08	–0.523		26.7		–0.52
4045.49	0.00	–0.933		27.3		–0.32
			ErII			
4023.00	0.21	–0.200		47.0		1.14
4043.59	0.32	–0.510		24.3		0.92
4051.14	0.38	0.090		39.5		0.80
4061.07	0.47	0.520		67.8		1.14
4109.44	0.00	–0.810		25.1		0.86
4113.83	0.18	–0.900		29.6		1.29
4133.35	0.32	–0.510		32.8		1.12
4156.07	0.18	0.180		69.9		1.17
4211.29	0.21	–0.720		30.0		1.15
4446.37	0.21	–0.590		46.5		1.38
4451.55	0.38	0.110		61.4		1.13
4451.98	0.00	–1.340		26.6		1.41
4567.60	0.21	–1.510		9.3		1.19
4579.32	0.74	–0.650		15.0		1.15
4645.77	0.56	–0.750		20.4		1.22
5092.78	0.38	–0.610		28.1		1.04
5192.62	1.14	0.310		35.2		1.10

TABLE 1
EQUIVALENT WIDTHS

λ Å	E.P. (eV)	log gf	Method	EW mÅ	HFS, IS?	log ϵ
5200.12	0.56	–0.490		10.7		0.56
5212.35	0.21	–0.870		24.2		1.02
			TmII			
3462.20	0.00	0.030	EW	32.5		–0.26
3700.26	0.03	–0.380	SYN	23.7		–0.20
3701.36	0.00	–0.540	SYN	16.6		–0.30
3761.91	0.00	–0.430	SYN	17.2		–0.40
			YbII			
3694.20	0.00	–0.229	SYN	118.6	HFS,IS	0.76
			LuII			
3507.32	0.00	–1.540	syn	51.4	HFS	–0.10
			HfII			
3253.70	0.38	–0.580	SYN	34.1		0.70
3389.83	0.45	–0.700	SYN	26.7		0.62
3399.79	0.00	–0.490	SYN	65.1	HFS,IS	0.64
3505.22	1.04	–0.080	SYN	30.2		0.70
3535.55	0.61	–0.540	SYN	29.1		0.67
3569.03	0.79	–0.400	SYN	27.7		0.67
3644.35	0.79	–0.480	SYN	25.5		0.67
3719.28	0.61	–0.870	SYN	26.5		0.82
3793.38	0.38	–0.950	SYN	25.0		0.60
3918.09	0.45	–1.010	SYN	23.4		0.67
4093.16	0.45	–1.090	SYN	26.8		0.82
			PbI			
3683.47	0.97	–0.790	EW	42.8	HFS,IS	2.43
4057.81	1.32	–0.481	EW	51.2	HFS,IS	2.48

[a]All abundances given as [Element/Fe], except for Fe where [Fe/H] is given.